Inelastic Lateral Torsional Buckling of Beam Columns

Flambage torsionnel latéral non-élastique de colonnes

Unelastisches seitliches Torsionsknicken von Stützen

G. ABDEL-SAYED
Associate Professor

A. A. AGLAN
Research Assistant

Department of Civil Engineering, University of Windsor

Introduction

A wide flange beam-column subjected to an axial force and to end moments about its major axis may fail because of: (1) local buckling, (2) excessive bending in the plane of applied moments, or (3) lateral torsional buckling. The local buckling can be avoided by satisfying specified width to thickness ratios of the cross-sectional components [8] which, fortunately, are usually met in most WF shapes. By eliminating the local buckling, the relationship between the applied end moment, M_0, and the resulting slope, θ, of a wide-flange member follows one of the curves shown in Fig. 1 in which the length as well as the axial force, P, are assumed to remain constant. The optimum performance of the beam-column is reached if failure is due to excessive bending in the plane of the applied moment [6, 9], i.e. curve (a) with maximum moment $\bar{M}_{0max}$. If no adequate lateral bracing is provided, the beam-column deflects laterally out of the plane of bending with simultaneous rotation before reaching its ultimate bending capacity. This behaviour starts at a bifurcation point B (see Fig. 1) beyond which the M-θ curve slopes slightly upwards indicating capability of the member to carry additional loading [7, 13]. However, this additional loading is so small that the bifurcation point is considered to effectively determine the buckling limit to the beam-column.

The problem of lateral torsional buckling of beam-columns has been extensively studied in the elastic range. In the inelastic range, it was examined by MIRANDA [12, 13], who took into account the prebuckling displacements of the column (i.e. the deflection in the plane of applied moment before the

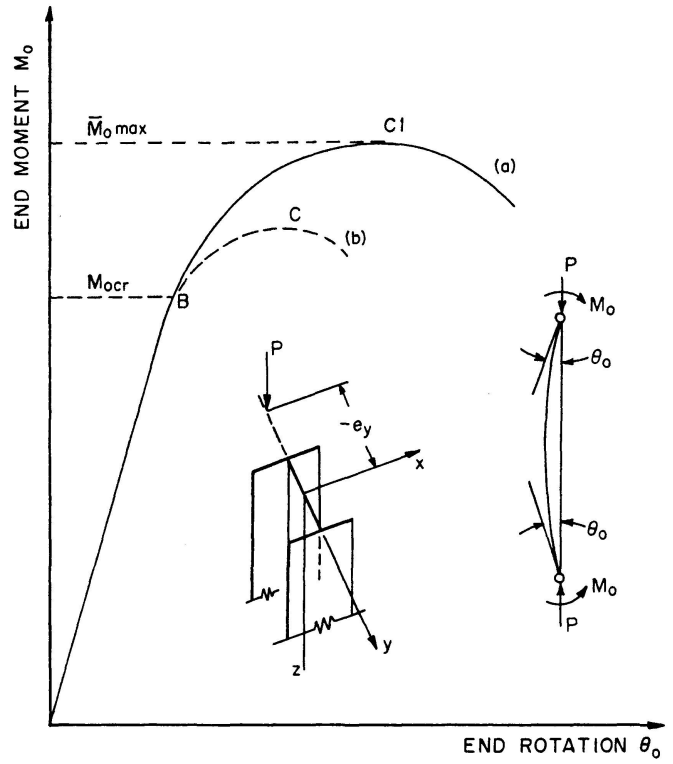

Fig. 1. Typical M-θ curves for a beam column under uniaxially eccentric load.

initiation of the lateral torsional buckling), but he neglected the residual stresses and the strain hardening. FUKUMOTO [4, 5] also examined this problem considering the residual stresses but neglecting the pre-buckling displacements as well as the strain hardening. The effect of strain hardening in the problem of lateral buckling of beam columns appears to have been neglected.

This study examines the problem of elastic and inelastic lateral-torsional buckling of perfectly straight wide-flange beam-columns subjected to axial force and equal end moments about the major axis. The residual stresses and pre-buckling displacements are considered together with the strain hardening.

Differential Equations

The differential equations governing the lateral torsional buckling of a beam-column have been treated extensively [4, 7, 14, 16] based on the following assumptions:

1. The beam-column is perfectly straight. The WF cross-section does not vary along the length of the beam and retains its original shape without distortion prior to and during buckling. The deflection and rotations are too small relative to the dimensions of the beam-column.

2. The axial force, P, and the end moments, M_0, are applied at the ends of the beam-column and no lateral forces are acting between the ends. The

moments, M_0, act about the major axis of the cross-section. The axial force acts along the direction of the original centroidal axis of the cross-section and retains its direction until failure.

The three simultaneous, differential equations which govern lateral torsional buckling are [13]:

$$B_x(v_i''+v'')+M_0+P(v_i+v)=0, \tag{1a}$$

$$B_y u''+Pu+[M_0+P(v_i+y_0)]\beta=0, \tag{1b}$$

$$C_w\beta'''-(C_T-\int_A \sigma r^2 dA)\beta'+[M_0+P(v_i+y_0)]u'=0, \tag{1c}$$

in which u, v = displacement in the x- and y-directions respectively; β = rotation about the z-axis; v_i = prebuckling displacement; B_x, B_y = flexural rigidity about the x- and y-axis respectively; C_T = St. Venant's torsional rigidity; C_w = warping rigidity; $\int_A \sigma r^2 dA$ = Wagner effect; y_0 = distance from centroid, c, to shear centre, s. The $'$, $''$ and $'''$ indicate the first, second and third differentiations with respect to z. Eq. (1a) governs the M-P-ϕ relationship occurring between the moment about the x-axis, $M^x=M_0+P(v_i+v)$, the thrust, P, and the curvature $\phi^x=v_i''+v''$. It is independent of the lateral displacement, u, and the torsional displacement, β; therefore, it has no effect on lateral-torsional buckling of elastic beam-columns. However, for inelastic beam-columns the M-P-ϕ relationship does affect the lateral torsional buckling as it governs the strain-distribution in cross-sections and the corresponding rigidity coefficients appearing in Eqs. (1b) and (1c).

Boundary Conditions

The ends of the beam-column are free to rotate about either principal axes with no displacement in either direction. They are also free to warp but their rotation about the longitudinal axis (z-axis) is prevented. These boundary conditions can be written as follows: at $z=0$ and $z=L$: $u=u''=\beta=\beta'=0$ in which L = the length of the beam column.

Material Properties

The idealized stress strain relationship of steel is shown in Fig. 2, it is the same for compression and tension stresses and can be formulated as follows:

$$\sigma = E\epsilon - E[\epsilon \pm \epsilon_y] + \left(\frac{E_{st}}{E}\right) E[\epsilon \pm \epsilon_{st}], \tag{2}$$

in which σ = the stress; E = modulus of elasticity; E_{st} = the strain hardening modulus; ϵ_y and ϵ_{st} = the absolute value of the yield strain and the strain at

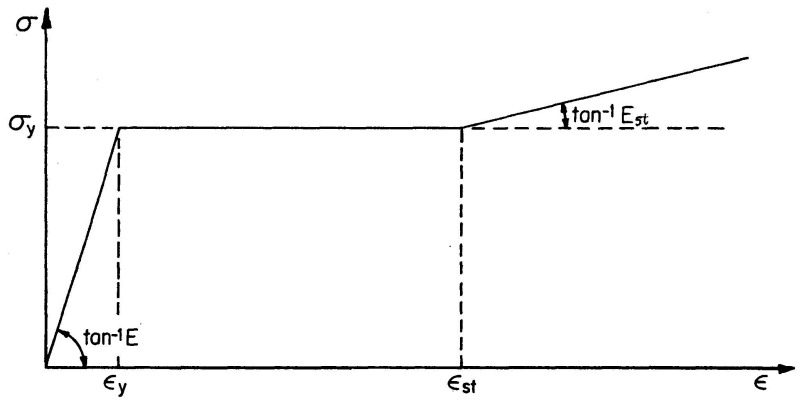

Fig. 2. Idealized stress-strain diagram (in tension and compression).

the onset of strain hardening. The two brackets have special significance as follows:

1. when $\epsilon < \epsilon_y$, both brackets disappear;
2. when $\epsilon_y < \epsilon < \epsilon_{st}$, only the second bracket disappears,
3. when $\epsilon_{st} < \epsilon$, both brackets are taken into consideration.

The signs inside the brackets are positive if ϵ is negative and vice versa.

The residual stresses are assumed to be distributed symmetrically about the y-axis as shown in Fig. 3 [10] and can be given by the following Eq.:

$$\sigma_R = \sigma_{rt} + \frac{\sigma_{rc} - \sigma_{rt}}{(b/2)} |x|, \tag{3}$$

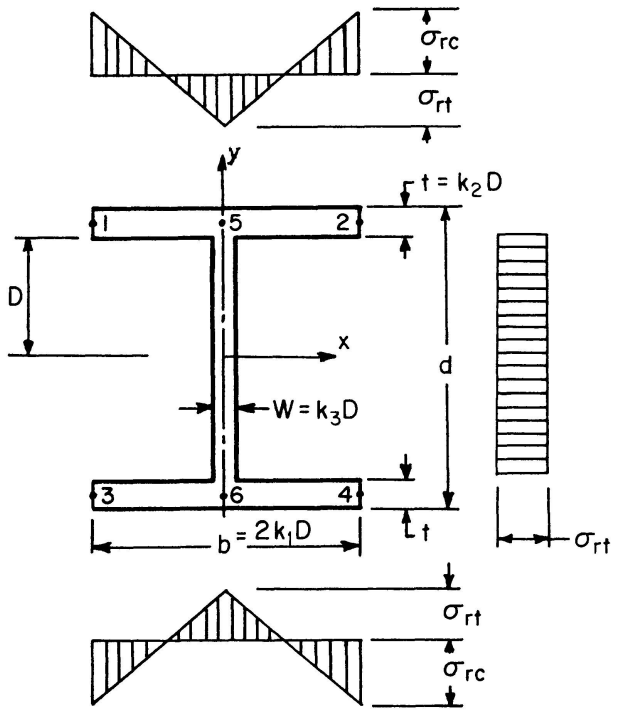

Fig. 3. Assumed residual stress pattern.

in which σ_{rc}, σ_{rt} = maximum compressive and tensile residual stresses respectively; b = the width of the flange and $|x|$ = the absolute value of x.

The residual stresses are always less than the yield stresses, therefore a corresponding residual strain can be introduced by dividing both sides of Eq. (3) by E, obtaining the following equation:

$$\epsilon_R = \epsilon_{rt} + \frac{\epsilon_{rc} - \epsilon_{rt}}{(b/2)} |x| . \tag{4}$$

Method of Solution

Based on the above definitions, equations and boundary conditions, the investigation of the lateral torsional buckling problem in a beam-column (i.e. the detection of the bifurcation point, B, on the M_0-θ curve, Fig. 1), then follows four steps:

I. Determination of Moment-Thrust-Curvature Relationship

This relationship, known as M-P-ϕ curves, is first established for a cross-section subjected to axial force, P, and a moment, M^x, acting about the x-axis. Plane cross-sections are assumed to remain plane after beam-column deformation; therefore, the strain at any point (x, y) on the cross-section can be written as follows:

$$\epsilon = \epsilon_0 + \phi^x y + \epsilon_R , \tag{5}$$

in which ϵ_0 = the average normal strain, i.e.

$$\epsilon_0 = \frac{1}{A} \int \epsilon \, dA . \tag{6}$$

ϕ^x = the curvature about the x-axis and $\phi^x y$ is the flexural strain referred to as ϵ_m ($\epsilon_m = \phi^x y$). The relatively small thickness of flanges and web (in comparison with the cross-section) insures that the strains can be safely assumed to be uniform over these thicknesses. The strains are symmetric about the y-axis and can take any one of the sixteen configurations shown in Fig. 4.

The equilibrium between external and internal forces requires that:

$$P = \int_A \sigma \, dA \tag{7}$$

and

$$M^x = \int_A \sigma y \, dA . \tag{8}$$

Substituting Eq. (2) in Eq. (7) and dividing by the axial thrust P_y which corresponds to the yield stress level, $P_y = E \epsilon_y A$, leads to:

$$\frac{P}{P_y} = \frac{1}{A} \int \frac{\epsilon}{\epsilon_y} dA - \frac{1}{A} \int \left[\frac{\epsilon}{\epsilon_y} \pm 1 \right] dA + \frac{1}{A} \left(\frac{E_{st}}{E} \right) \int \left[\frac{\epsilon}{\epsilon_y} \pm \frac{\epsilon_{st}}{\epsilon_y} \right] dA . \tag{9}$$

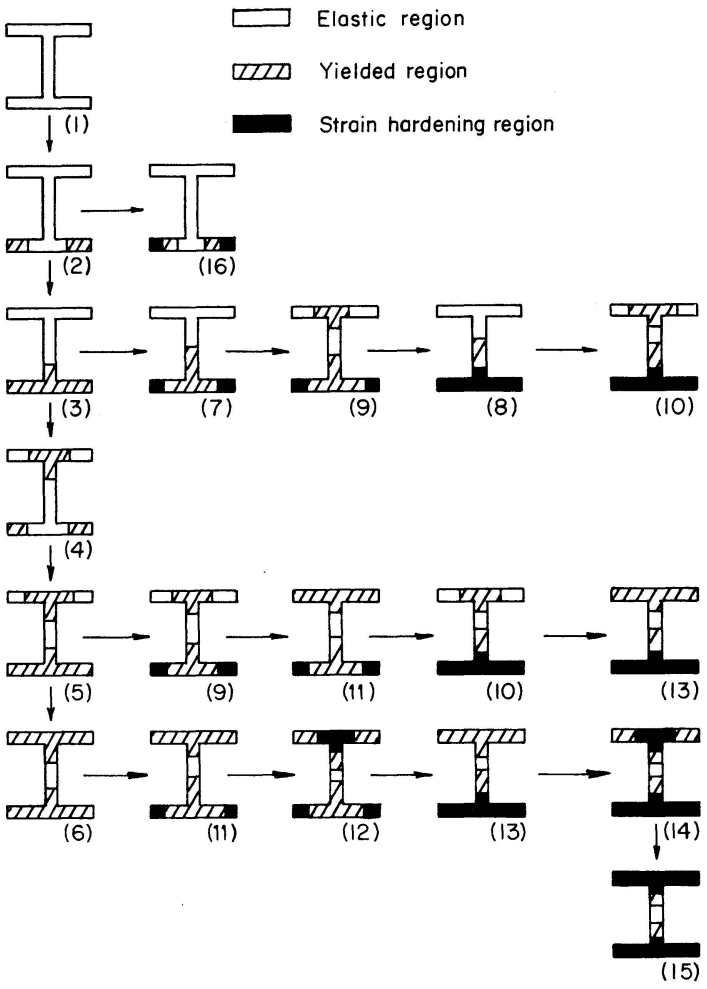

Fig. 4. Sequence for checking the strain patterns.

The first integral of Eq. (9) equals to ϵ_0/ϵ_y (Eq. (6)) in the non-dimensional form, while the second and third integrals are the sectional volumes of $\left[\frac{\epsilon}{\epsilon_y} \pm 1\right]$ and $\left[\frac{\epsilon}{\epsilon_y} \pm \frac{\epsilon_{st}}{\epsilon_y}\right]$ respectively and can be calculated numerically for any assumed strain configuration. Therefore, Eq. (9) takes the form:

$$Q\left(\frac{\epsilon_0}{\epsilon_y}\right)^2 + R\left(\frac{\epsilon_0}{\epsilon_y}\right) + S = 0, \tag{10}$$

in which Q, R and S are coefficients depending on the thrust P, flexural strains ϵ_m, geometry of section, residual stresses and the assumed strain configuration. Expressions for Q, R and S have been derived in Reference [2].

Using non-dimensional factors K_1, K_2 and K_3 to describe the cross-section as shown in Fig. 3 and substituting Eq. (2) in Eq. (8) and dividing by the moment M_y^x at which yielding first occurs in flexure, leads to:

$$\frac{M^x}{M_y^x} = \frac{D(1+K_2)}{I^x}\left\{\int_A y\left(\frac{\epsilon}{\epsilon_y}\right) dA - \int_A y\left[\frac{\epsilon}{\epsilon_y} \pm 1\right] dA + \left(\frac{E_{st}}{E}\right)\int_A y\left[\frac{\epsilon}{\epsilon_y} \pm \frac{\epsilon_{st}}{\epsilon_y}\right] dA\right\}, \tag{11}$$

in which the integrals on the left hand side can be calculated numerically for any assumed strain configuration (D = half depth of the web).

For a specified thrust P and residual stress distribution, a trial and error procedure is applied [2, 11].

1. A curvature ϕ^x is assumed and the flexural strains, $\epsilon_m = \phi^x y$ are calculated at the points 1 to 6 shown in Fig. 3.
2. A strain configuration is assumed and with the flexural strains ϵ_m calculated in step No. 1, the coefficients Q, R and S are calculated for the specified thrust P and residual stresses.
3. Q, R and S are substituted in Eq. (10) and ϵ_0/ϵ_y is calculated.
4. The strain is calculated using Eq. (5). The corresponding strain configuration is found and compared with the assumed one.
5. The steps 1 to 4 are repeated until the calculated configuration becomes the same as the assumed one, then the moment M^x is calculated using Eq. (11). Since this moment corresponds to the assumed curvature ϕ^x and thrust, P, it presents a point on the M-P-ϕ curve.
6. Repeat steps 1 to 5 for different curvatures ϕ^x and find the corresponding moments M^x.

II. Determination of the Cross-Sectional Mechanical Properties

The cross-sectional properties B_y, C_w, y_0 and $\int \sigma r^2 dA$, which are constant along the length of an elastic beam-column, become variable in the inelastic range because of partial yielding or strain-hardening. The bending and warping rigidities are the elastic rigidities of the unyielded part of cross-section plus the rigidities of the strain hardening area. The distance y_0 is calculated between the original centroid of the section and the shear centre of the unyielded area. Formulas are established [2] for the B_y, C_w and y_0 for each of the strain configuration, Fig. 4.

The derivation of mathematical expression for the Wagner effect becomes too laborious for inelastic sections. Therefore, it is calculated numerically by dividing each flange and web to 20 equal parts [2]. The St. Venant torsional rigidity, in line with previous studies [3, 4, 7, 13, 14] is assumed to be always equal to the elastic torsional rigidity.

III. Determination of End-Moment Versus End-Rotation

For a beam-column with specified length, L, thrust, P, and end moments M_0, a deflection curve can be obtained using numerical integration and the M-P-ϕ curves developed in phase I. The end moments are equal; therefore, the deflection curve is symmetrical with zero slope at the middle where the integration starts. From a group of column deflection curves (*CDC-S*) the curves of end-moment versus end rotation can be obtained [15].

IV. Determination of the Lateral-Torsional Buckling

Each point on the M_0-θ curve, Fig. 1, represents a stable, uni-axially loaded beam-column deflected in the plane of applied end-moments. The deflection curve and bending moments diagram is defined in phase III. With specified thrust and moment, any cross-sectional strain-configuration can be obtained from phase I and the mechanical properties calculated in phase II.

The lateral torsional buckling (bifurcation point, B) is examined using Eq. (1b) and Eq. (1c) where coefficients (beam-column's sectional-properties) are variable with respect to z. Therefore, a direct solution is rather difficult and a finite difference approximation is applied. This leads to a set of simultaneous algebraic equations in the lateral displacement u and the rotations β at a number of discrete points spaced at $h = L/n$, in which n is an odd number to which the beam is divided (5).

This system of equations can be written in matrix form as follows:

$$(C - \lambda I) X = 0, \tag{12}$$

in which C = real non-symmetric matrix, λ = eigenvalues, $(\lambda = 1 - M_{0i})$, I = identity matrix and X = eigenvectors.

The point of onset of lateral-torsional buckling and the rigidity coefficients (B_y, C_T, C_w, y_0 and $\int \sigma r^2 dA$) are interdependent. Therefore, a trial and error approach is applied to solve the problem.

A critical end-moment, M^1_{0i}, is assumed using an approximate method for a beam-column with specified length and axial load, P. The deflection and the moment at evenly spaced discrete points along the entire length of the beam-column can be calculated using the *CDC-S* (phase 3). The corresponding mechanical properties are calculated from phase 2 for the section at each of the discrete points. The matrix C can then be calculated and also the corresponding minimum critical end moment, M_{0i}, from the eigenvalues of matrix C. M_{0i} is then compared with the assumed M^1_{0i}. If the ratio $\frac{M_{0i}}{M^1_{0i}}$ is different from unity, the procedure is repeated until M^1_{0i} assumed becomes close enough to the calculated M_{0i}.

A computer programme for all the theoretical work of the four phases has been written for the IBM system 360/50 at the University of Windsor.

Observations

1. An example of an 8 *WF* 31 is investigated and the results are compared with previously published results as follows:

a) The theoretically obtained results of references [5, 13] are in good agreement with the results of the present investigation when the same assumptions are taken into consideration.

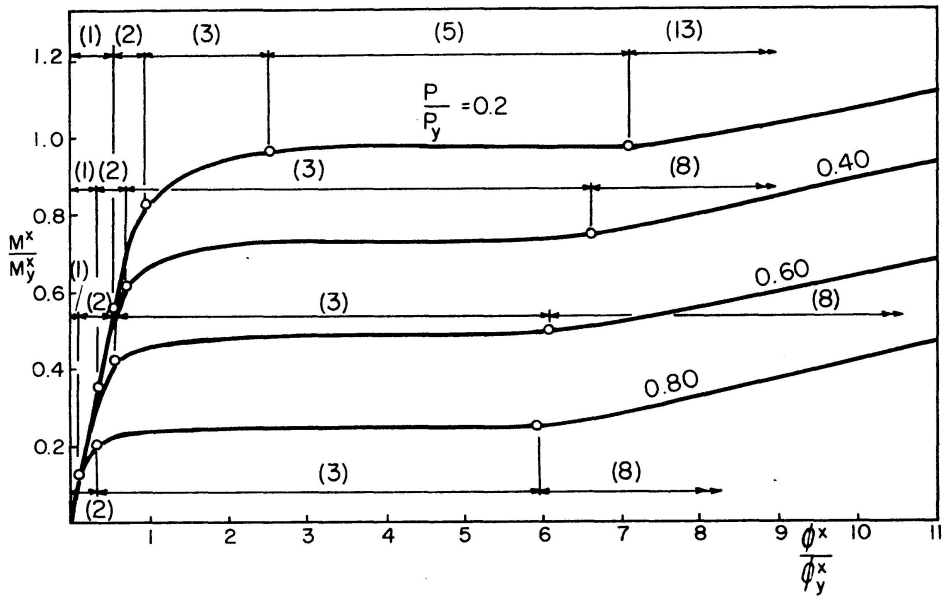

Fig. 5. Moment-curvature-thrust relationship for 8WF31 ($\sigma_y=36$, $E_{st}/E=0.022$ and $\epsilon_{st}/\epsilon_y=12$).

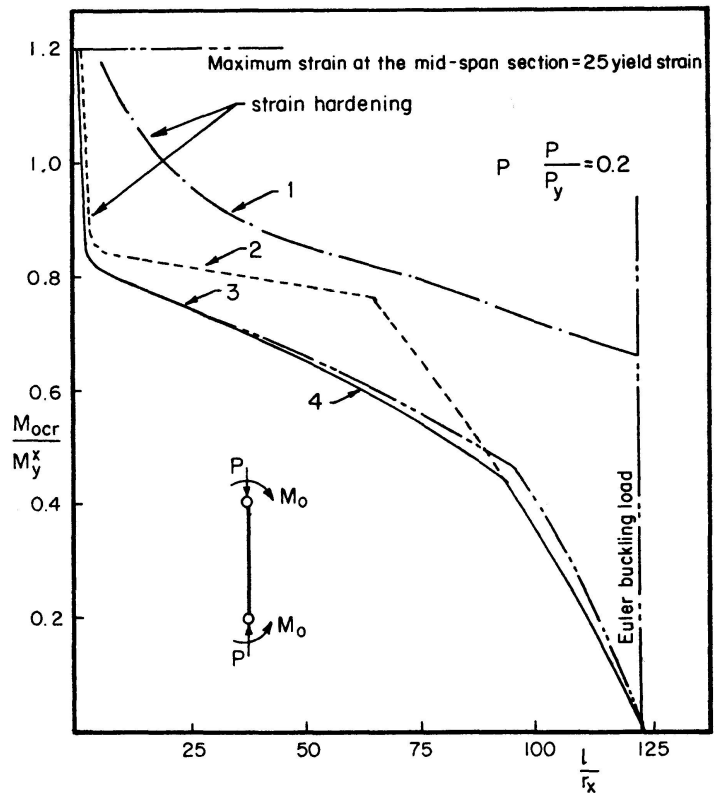

Fig. 6a. Lateral torsional buckling strength curves for a 8 WF 31 ($\sigma_y=36$, $E_{st}/E=0.022$ and $\epsilon_{st}/\epsilon_y=12$).

1 Failure by excessive bending considering residual stresses – 2, 3, 4 Failure by lateral torsional buckling – 2 neglecting residual stresses – 3 neglecting pre-buckling displacements – 4 considering residual stresses and pre-buckling displacements.

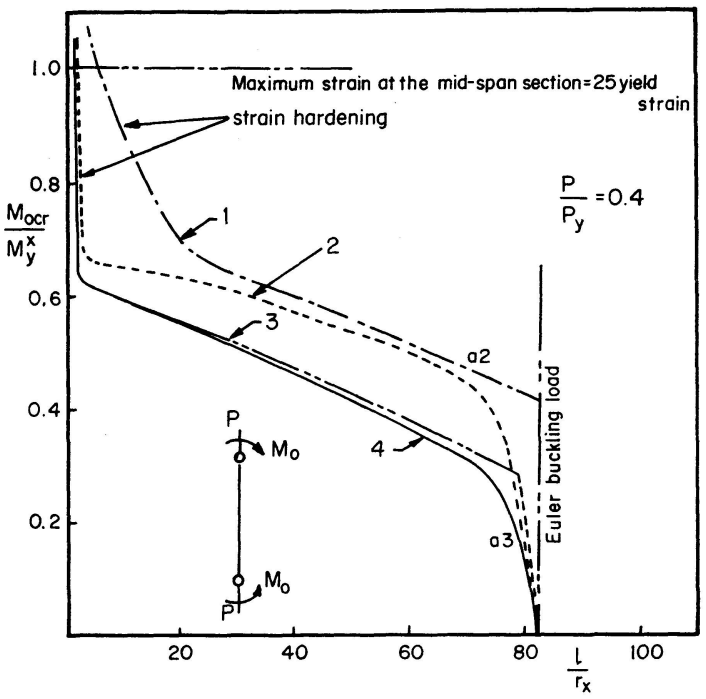

Fig. 6b. Lateral torsional buckling strength curves for a 8 WF 31 ($\sigma_y = 36$, $E_{st}/E = 0.022$ and $\epsilon_{st}/\epsilon_y = 12$).

1 Failure by excessive bending considering residual stresses – 2, 3, 4 Failure by lateral torsional buckling – 2 neglecting residual stresses – 3 neglecting pre-buckling displacements – 4 considering residual stresses and pre-buckling displacements.

b) The experimentally obtained results of reference [7] for $\frac{P}{P_y} = 0.12$ show good agreement with the present investigation.

2. The domains of the different strain configurations is shown in Fig. 5 of the M-P-ϕ relationships. They indicate that for $\frac{P}{P_y} = 0.4$ to 0.8 the prevalent configurations are numbers 1, 2 and 3 for the elastic and plastic ranges followed by configuration 8 for the strain hardening range. With low ratio of $\frac{P}{P_y}\left(\frac{P}{P_y} = 0.2\right)$ the configurations are numbers 1, 2, 3, 5 and 13. These results help in executing phase I by assuming the most probable strain configuration.

3. The effect of residual stresses, pre-buckling deflection, and strain hardening can be seen in Figs. 6a, b, c for $\frac{P}{P_y} = 0.2$, 0.4 and 0.6. The curves in each figure relate the $\left(\frac{M_0}{M_y^x}\right)$ to the slenderness rate $\left(\frac{L}{r_x}\right)$. Curve 1 is for failure due to excessive bending and considering residual stresses. Curves 2, 3 and 4 illustrate failure due to lateral torsional buckling with curve 2 for neglected residual stresses and considered pre-buckling, curve 3 for considering residual stresses and neglecting pre-buckling and curve 4 for both considered residual stresses anp pre-buckling displacements.

Each of the curves is seen to be built of elastic, plastic and strain hardening

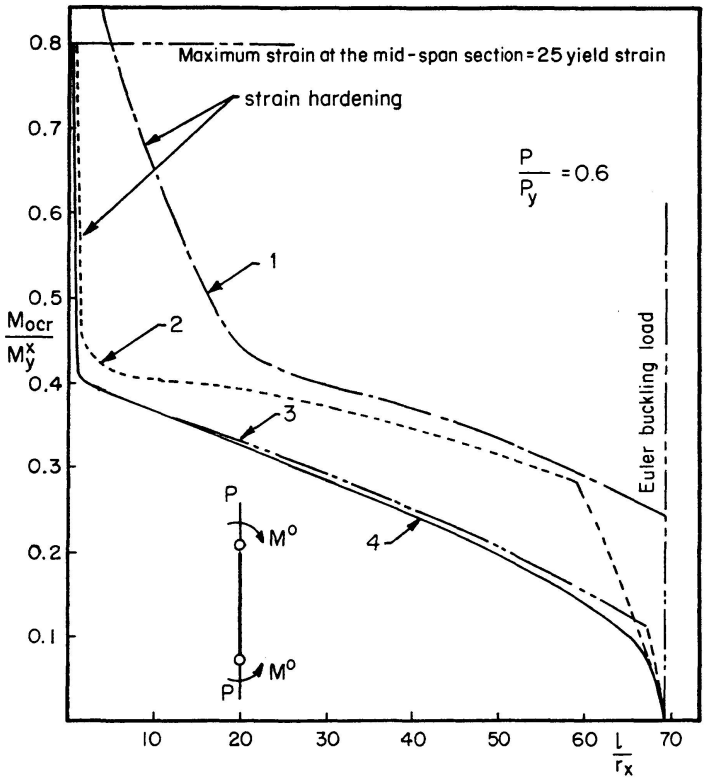

Fig. 6c. Lateral torsional buckling strength curves for a 8 WF 31 ($\sigma_y = 36$, $E_{st}/E = 0.022$ and $\epsilon_{st}/\epsilon_y = 12$).

1 Failure by excessive bending considering residual stresses – 2, 3, 4 Failure by lateral torsional buckling – 2 neglecting residual stresses – 3 neglecting pre-buckling displacements – 4 considering residual stresses and pre-buckling displacements.

ranges. The effect of the residual stresses, pre-buckling, and strain hardening can be discussed further as follows:

a) Effect of Pre-Buckling Displacement

The pre-buckling displacement v_i appears in the differential equation added to y_0 and multiplied by P, $P(v_i + y_0)$. This term is proportional to the loading, therefore calculating the pre-buckling has relatively small effect for small ratios of $\frac{P}{P_y}$ curve (see Figs. 6a, b, c), its effect disappears completely when $\frac{P}{P_y} = 0$. For a constant ratio $\frac{P}{P_y}$, the displacement v_i is greater than y_0 in the elastic range while v_i is too small when compared to y_0 in the inelastic range. Therefore, the buckling load calculated with the pre-buckling displacement v_i has maximum reduction in the elastic range (Figs. 6a, b, c). Compare curve 4 with curve 3.

b) Effect of Residual Stresses

Figs. 6a, b, c show that residual stresses has negligible effect on the lateral torsional buckling in the elastic range. However, they reduce the maximum moment that can be reached before the start of the inelastic range (compare

point a_2 with point a_3 in Fig. 6b). Within the inelastic range, the residual stresses have considerable effect on the lateral torsional buckling because they extend the yielding zone in the cross-section leading to reduction in the bending and warping rigidities.

c) Effect of Strain Hardening

The present analysis is for mild steel, with $\frac{\epsilon_{st}}{\epsilon_y} = 12$; the maximum strain in the strain hardening range is limited to twelve times the yield strain, ϵ_y. The strain hardening has an effect only in short columns where $\frac{l}{r_x} < 8$. Such short columns are of little practical interest. However, for high tensile steel or aluminium alloy with stress-strain relationship different from that of mild steel, i.e. $\frac{\epsilon_{st}}{\epsilon_y} < 12$ and/or $\frac{E_{st}}{E} > 0.022$, the effect of strain hardening will be considerable and extends to slender columns.

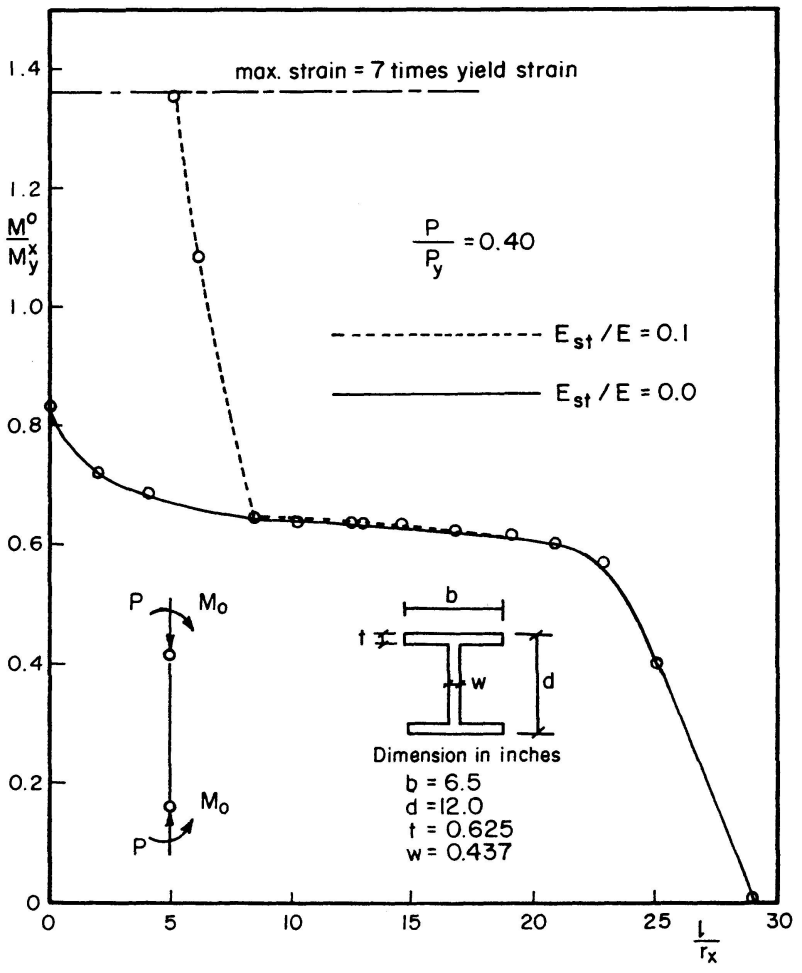

Fig. 7. Lateral torsional buckling strength curves for an aluminium alloy section Alcan No. 28021. Comparing the Calculations with $E_{st}/E = 0.10$ and 0.0.

(Considering pre-buckling displacement and assuming no residual stresses, $\sigma_y = 27$ ksi, $E = 10{,}000$ ksi, $\epsilon_{st}/\epsilon_y = 1.0$).

To investigate the effect of the ratio $\frac{E_{st}}{E}$ on the lateral torsional buckling strength, an aluminium alloy section (Alcan 28021) is examined considering $\frac{E_{st}}{E}=0.1$ and 0.0 and $\frac{\epsilon_{st}}{\epsilon_y}=1.0$. A comparison of the two curves in Fig. 7 shows that the strain hardening has appreciable effect on the lateral torsional buckling.

Conclusions

This paper examines the problem of lateral torsional buckling of uniaxially loaded beam-columns. The main points of conclusion are:

1. The lateral torsional buckling reduces the strength of beam-columns considerably in the inelastic range.

2. Residual stresses have negligible effect on the buckling load in the elastic range but they reduce the buckling load considerably in the inelastic range.

3. The effect of pre-buckling displacements is not always insignificant and being neglected may lead to considerable errors on the unsafe side.

4. The strain hardening of mild steel has appreciable effect only on short columns (where $\frac{l}{r_x}<8$).

Acknowledgement

Appreciation is expressed to the National Research Council of Canada for financial support for this work under Grant No. A-4350.

Notation

The following symbols are used in this paper:

A = area of cross section;
B_x, B_y = bending rigidity about the x- and y-axis respectively;
b = width of flange;
$[C]$ = square matrix;
C_T = St. Venant's torsional rigidity;
C_w = Warping rigidity;
d = depth of wide-flange section;
D = half depth of the web;
E = modulus of elasticity;
E_{st} = strain hardening modulus;
$[I]$ = identity matrix;
K_1, K_2, K_3 = factors defining the dimensions of the cross-section (see Fig. 3);
L = length of the beam-column;
M_0 = applied end moment

M_{cr} = actual critical end moment;
M_{0i} = calculated critical end moment;
M_{0i}^{1} = assumed critical end moment;
$\overline{M}_{0\,max}$ = maximum end moment due to lateral torsional buckling;
M^x = applied moment on a section about the x-axis;
M_y^x = applied moment on a section at which yielding first occurs in flexure ($P=0$);
P = axial load;
P_y = axial load causing yielding over the entire cross-section;
r_x = radius of Gyration about x-axis;
t = flange thickness;
u, v = displacements in the x- and y-directions;
v_i = pre-buckling displacements in the plane of the applied moment;
w = web thickness;
x, y, z = system of axis used;
$|X|$ = matrix containing eigenvectors;
y_0 = distance from the centroid, to the shear center;
β = rotation of the cross-section about the shear center;
ϵ = axial strain;
ϵ_0 = strain corresponding to the axial force, P;
ϵ_m = axial strain due to bending;
ϵ_R = residual strain;
ϵ_{rc} = maximum compressive residual strain;
ϵ_{rt} = maximum tensile residual strain;
ϵ_{st} = strain at the onset of the strain hardening;
ϵ_y = yield strain;
σ = stress;
σ_R = residual stress;
σ_r = maximum compressive residual stress;
σ_r = maximum tensile residual stress;
ϕ^x = curvature about the x-axis;
ϕ_y^x = curvature about the x-axis corresponding to initial outer fiber yielding ($P=0$);
$[\lambda]$ = matrix containing eigenvalues;
θ = end rotation;
$\int_A \sigma r^2 dA$ = Wagner effect.

References

1. ADAMS, PETER F., and GALAMBOS, T. V.: Material Considerations in Plastic Design. International Association for Bridge and Structural Engineering, Vol. 29-II, 1969.
2. AGLAN, A. A.: The Ultimate Carrying Capacity of Beam Columns. Thesis presented to the University of Windsor, at Windsor, Ontario, in partial fulfillment of the requirements for the degree of Doctor of Philosophy, 1972.
3. BAKER, J. F., HORNE, M. R., and HEYMAN, J.: The Steel Skeleton. Vol. 2, Cambridge University Press, 1956.
4. FUKUMOTO, YUHSHI: Inelastic Lateral-Torsional Buckling Under Moment Gradient. Thesis presented to Lehigh University, at Betlehem, Pa., in 1963, in partial fulfillment of the requirements for the degree of Doctor of Philosophy, 1972.
5. FUKUMOTO, YUHSHI, and GALAMBOS, T. V.: Inelastic Lateral-Torsional Buckling of Beam-Columns. Journal of the Structural Division, ASCE, Vol. 92, No. ST 2, proc. paper 4770, April, 1966.
6. GALAMBOS, T. V. and KETTER, R. L.: Columns Under Combined Bending and Thrust. ASCE Trans., Vol. 126, Part I, p. 1, 1961.
7. GALAMBOS, T. V.: Inelastic Lateral-Torsional Buckling of Eccentrically Loaded WF Columns. Ph. D. Dissertation, Lehigh University, 1959.
8. HAAIJER, G.: On Inelastic Buckling in Steel. Journal of the Engineering Mechanics Division, ASCE, Vol. 84, No. EM 2, Proc. paper 1581, April, 1958.
9. KETTER, R. L.: Further studies on the Strength of Beam-Columns. Journal of the Structural Division, ASCE, Vol. 87, No. ST 6, Proc. paper 2910, August 1961.
10. KETTER, R. L., and KAMINSKY, E. L., and BEEDLE, L. S.: Plastic Deformations of Wide-Flange Beam-Columns. Transactions, ASCE, Vol. 120, 1955, P. 1028.
11. MCVINNIE, W. W.: Elastic and Inelastic Buckling of an Orthogonal Space Frame. Thesis submitted to the University of Illinois, in 1966, in partial fulfillment for the degree of Doctor of Philosophy.
12. MIRANDA, CONSTANCIO, and OJALVO, MORRIS: Inelastic Lateral-Torsional Buckling of Beam-Columns. Journal of the Engineering Mechanics Division, ASCE, Vol. 91, No. EM 6, proc. paper 4563, December 1965.
13. MIRANDA, CONSTANCIO: The Occurrence of Lateral-Torsional Buckling in Beam-Columns. Thesis presented to the Ohio State University at Columbus, Ohio, in 1964, in partial fulfillment of the requirements for the degree of Doctor of Philosophy.
14. NEAL, B. G.: The Lateral Instability of Yielded Mild Steel Beams of Rectangular Cross Section. Phil., Trans. of Royal Society, Vol. 242, Series A, January 1950.
15. OJALVO, MORRIS: Restrained Columns. Journal of the Engineering Mechanics Division, ASCE, Vol. 86, No. EM 5, proc. paper 2615, October 1960, p. 2.
16. TIMOSHENKO, S. P., and GERE, J. M.: Theory of Elastic Stability. McGRAW-Hill Book Co., Inc., New York, N. Y. 1961.
17. WAGNER, H.: Torsion and Buckling of Open Sections. N.A.C.A. Tech. Mem. No. 807, 1936 (Translation).
18. WATTRICK, W. H.: Lateral Instability of Rectangular Beams of Strain Hardening Material Under Uniform Bending. Journal of Aeronautical Science, 19 (12), 835, December 1952.

Summary

The problem of elastic and inelastic lateral-torsional buckling is examined for perfectly straight wide-flange beam-columns subjected to axial force and equal end moments about the major axis. The residual stresses and pre-buckling displacements are considered together with the strain hardening. The investigation is conducted using finite difference approximation and trial and error procedure.

Résumé

Le problème du flambage élastique et non élastique latéral et torsionnel est étudié pour des colonnes droites à larges semelles, exposées à des forces axiales et à des moments égaux dans l'axe majeure. On y tient compte des tensions résiduelles et des déplacements de préflambage ensemble avec le durcissement à l'allongement. L'étude est faite en utilisant les différences finies approchées et la méthode d'essais et des défauts.

Zusammenfassung

Das Problem des elastischen und unelastischen seitlich-torsionellen Knikkens wird für vollkommen gerade breitflanschige Stützen untersucht, die axialen Kräften und gleichen Endmomenten in der längeren Achse ausgesetzt sind. Dabei werden die Restspannungen und Vorknick-Verschiebungen zusammen mit der Streckhärtung betrachtet. Die Untersuchung wird unter Benützung der endlichen Differenzen-Annäherung und der Versuchs- und Fehlermethode durchgeführt.